Optimal design procedure of dual-reflux pressure swing adsorption units for nonlinear separations

Ester Rossi[a], Giuseppe Storti[b], Renato Rota[a,]*

[a] Chemistry, Materials and Chemical Engineering Department "Giulio Natta", Politecnico di Milano, Via Mancinelli 7, 20131 Milan, Italy

[b]ETH Zürich, Department of Chemistry and Applied Biosciences, Vladimir-Prelog-Weg 1-5/10, HCI F 125, 8093 Zürich, Switzerland

Abstract

In the frame of dual-reflux pressure swing adsorption processes, design strategies applicable to the complete separation of binary gas mixtures are available only in the case of linear adsorption isotherms. Therefore, in this work we propose a simple and efficient design procedure which enables the selection of suitable operating conditions when sharp separation is required and Langmuir adsorption isotherms are involved. Starting from the available strategy for the linear adsorption case, we adapt it to the non-linear case tuning properly the pressure ratio. Then, the resulting design strategy is validated by application to selected study cases involving different values of key parameters such as different levels of non-linearity of the isotherms, but also different values of pressure ratio, feed composition and selectivity.

Keywords

Dual-reflux; PSA design; Gas separation; Cyclic adsorption process; Detailed numerical modelling; Non-linear adsorption;

Symbols

A	Heavy component
a_i	Langmuir coefficient, component i
B	Light component
b_i	Langmuir coefficient, component i
BD	Blowdown step
$\mathbb{C}$	Capacity Ratio

D_L Diffusivity coefficient $[m^2/s]$

D Diameter of the adsorption bed

d_p Diameter of the solid particles

f Variable flowing through the finite volume walls

FE Feed step

$\mathbb{G}$ Reflux ratio

k_i Linear isotherm constant for component i

k_{LDF} Linear Driving Force constant

L Bed length

$\dot{n}$ Molar flowrate

n_F Computational node corresponding to the lateral feed injection position

$\dot{n}_F$ Lateral feed flowrate

$\dot{n}_H$ Heavy component flowrate $\dot{n}_H = \dot{n}_{HP} + \dot{n}_{HR}$

$\dot{n}_{HP}$ Heavy product flowrate

$\dot{n}_{HR}$ Heavy recycle flowrate

$\dot{n}_L$ Light component flowrate $\dot{n}_L = \dot{n}_{LP} + \dot{n}_{LR}$

$\dot{n}_{LP}$ Light product flowrate

$\dot{n}_{LR}$ Light recycle flowrate

P Pressure

$\bar{P}$ Pressure, dimensionless

PR Pressurization step

PU Purge step

q_i Amount of i on the solid adsorbent

$\bar{q}_i$ Amount of i on the solid adsorbent, dimensionless

q_i^* Amount of i on the solid adsorbent in equilibrium conditions

R Ideal gas constant

R_L Light recycle ratio

r_p Particle radius

T Temperature

t Time

$\bar{t}$ Time, dimensionless

u Superficial velocity

$\bar{u}$ Superficial velocity, dimensionless

$y_{i,F}$ Molar fraction of i in the lateral feed injection flow

$y_{i,H}$ Average molar fraction of i in ϑ_2

$y_{i,L}$ Average molar fraction of i in ϑ_1

y_i Molar fraction of i

z_F Feed injection position, dimensionless

z_F^- z coordinate of the outlet of Bed 1 Bottom

z_F^+ z coordinate of the inlet of Bed 1 Top

z Axial coordinate, dimensionless $z = Z/z_{ref}$

Z Axial coordinate

Greek symbols

β Selectivty

ε_{MB} Error on the material balance

ϵ_B Bed void fraction

ϵ_T	Total void fraction
ϵ_P	Solid particles porosity
ρ_s	Solid density
ρ_B	Bed density
μ	Dynamic viscosity
π	High pressure to low pressure ratio
ϑ_1	Tank 1
ϑ_2	Tank 2
α	Tolerance for the CSS reaching

Acronyms

PSA	Pressure Swing Adsorption
DR-PSA	Dual Reflux-Pressure Swing Adsorption
FVM	Finite Volume Method
PDE	Partial Differential Equation
ODE	Ordinary Differential Equation
PR	Pressurization step
FE	Feed step
PU	Purge step
BD	Blowdown step
BC	Boundary Condition

Subscripts

i	Component i, $i = A$ or B

n	n^{th} computational node, $n = 1 \dots N$
A	Heavy component
B	Light component
ref	Reference value
$n \pm \frac{1}{2}$	Walls of the computational nodes n
BD	Blowdown step
FE	Feed step
PR	Pressurization step
PU	Purge step
H	Highest value of the cycle
L	Lowest value of the cycle
Hen	Henry isotherm
Lan	Langmuir isotherm

1. Introduction

Pressure Swing Adsorption (PSA) can be employed to separate a gas mixture exploiting the different affinity of the components for a solid adsorbent [1-3]. The simplest configuration of this process involves two identical beds packed with a solid adsorbent. The gas mixture flows through one bed undergoing adsorption, while the other bed undergoes regeneration. The essential feature of PSA is that, once the solid adsorbent inside the adsorption bed is saturated, the feed is interrupted and the bed pressure is reduced [4]. The pressure reduction results in partial desorption of the species loaded in the saturated bed, which is further regenerated by flowing a suitable purge gas through it. The standard formulation of the process, known as stripping PSA, is based on the Skarstrom cycle [5]. When considering a binary mixture, a single product stream is collected at high purity of light species (which is the less adsorbed component, B), while the second product stream is only enriched in the heavy component (which is the strongly adsorbed one, A). Another configuration has been proposed, called enriching PSA [6]. Differently from the stripping one, the enriching PSA ensures component A only at high purity. In both configurations, a thermodynamic constraint limits the maximum purity of either the heavy or the light component [7].

To overcome this inherent limitation of the traditional PSA processes, in 1992 Leavitt [8] patented the so-called Dual Reflux-Pressure Swing Adsorption (DR-PSA) process. The main idea was to combine the two aforementioned process configurations, $i.e.$, the rectifying and the enriching PSA. This combination is obtained by carrying out the injection of the feed stream in an intermediate position of the columns, which divides each bed into an enriching and a rectifying section. Moreover, the DR-PSA process involves both a light and a heavy recycle: the first is used to purge the saturated bed and to recover the heavy component, A, while the second is fed to the bed during the adsorption step to enhance the desorption of the light component, B. Together with the pressure switching and the lateral feed injection, the two refluxes enable the achievement of the complete separation of a gas binary mixture [9]. Depending on the pressure of the bed receiving the lateral feed injection, two different process configurations exist, one with the feed at low pressure and the other at high pressure. Moreover, the pressure equalization can be carried out either using the heavy or the light product, thus providing four basic configurations of the DR-PSA process [10].

The opportunity of obtaining two pure products through a rather simple process has encouraged many experimental [11-19] and numerical [1, 9, 10, 16, 17, 20-23] investigations. Due to the complexity of the detailed mathematical modeling of the DR-PSA dynamics, the semi-analytical solution based on

Equilibrium Theory [6,24], represents also a valuable tool, previously applied to better understand the process [9, 10, 20, 21]. On the other hand, such solution relies on many simplifying assumptions: (i) linear adsorption isotherms, (ii) instantaneous equilibrium between solid and gas phases, (iii) ideal gas behaviour, (iv) complete separation of a binary mixture, (v) ideal plug flow (no axial mixing), (vi) isothermal operation and (vii) negligible pressure drops. Relying on this approach, Kearns and Webley [10] identified the relevance of the concentration of heavy component in the feed when choosing the dual-reflux configuration. Moreover, Bhatt and co-workers [20, 21] indicated how to identify the optimal feed location and define the operating region inside which complete separation at Cyclic Steady State (CSS) can be achieved. Even though this information is extremely helpful to identify the achievable separation performances, the many assumptions underlying the solution based on *Equilibrium Theory* limit its applicability, in particular with respect to the requirement of linear adsorption isotherms. In fact, when increasing the system pressure, most systems show deviations from the linear behaviour, thus preventing the design of the separation conditions based on this approach.

When such assumptions do not apply, general guidelines for the design of best operating conditions for a DR-PSA process are not available. In these cases, detailed mathematical modelling of the process is the only option and, in fact, this approach has been applied in several papers. For instance, in the case of the purification of natural gas with carbon capture, Kim and co-workers [23] proposed an optimisation framework for the purification through DR-PSA. In particular, each unit of the process, whose dynamics was simulated through a detailed model, was individually optimised with different objectives and constraints. May and co-workers [17] focused on the heavy product-to-feed ratio as a key cycle parameter to be tuned in DR-PSA units in order to improve the stripping or the enrichment. Finally, Sivakumar and Rao [22, 25] proposed a modified configuration for the DR-PSA process with the aim of enhancing the performances in the frame of CO_2/N_2 and N_2/O_2 separations. These contributions succeeded in identifying a suitable operating window for the specific process investigated combining detailed models with a trial-and-error procedure.

The aim of this work is to develop a design strategy combining the effective part of both approaches, that is, the numerical solution of a detailed model of the unit (removing most of the simplifying assumptions mentioned above) along with the information provided by the *Equilibrium Theory*. This methodology will be discussed with reference to systems governed by Langmuir isotherms, using the pressure ratio as design parameter to “compensate” for the nonlinearity of the adsorption

isotherm. Then, the novel design strategy will be applied to selected study cases involving different values of key parameters, such as different levels of non-linearity of the isotherms, but also different values of pressure ratio, feed composition and selectivity.

2. Process configuration and simulation

Let us focus on the DR-PH-A cycle, *i.e.* feed at the high pressure column and pressure swing using the stream rich in the heavy component. This process configuration was simulated through the conceptual scheme shown in Figure 1. The cyclic process involves two identical adsorption beds, Bed 1 and Bed 2. Each cycle consists of four steps, two of which are simultaneously performed at constant pressure (FE, feed step at high pressure and PU, purge step at low pressure) while the other two, again simultaneously, at varying pressure (PR, pressurization step, where the bed pressure changes from P_L to P_H, and BD, blowdown step, where the pressure changes from P_H to P_L). Therefore, the two beds are phase shifted by half a cycle: Figure 1 shows one-half of a complete cycle, while the second half is achievable just exchanging the two beds. Both columns are divided into two portions according to the feed position, identified by the value of the dimensionless coordinate $z = z_F$. Therefore, the section above the feed position ($z_F < z \leq 1$) is the *Rectifying* section and the one below ($0 \leq z < z_F$) the *Stripping* (or enriching) section. Note that two buffer tanks, ϑ_1.and ϑ_2, are also represented in Figure 1, whose primary role is to dampen the composition oscillations taking place during the cycle. Moreover, tank ϑ_2 is also necessary as buffer during the variable pressure steps since the amount of gas leaving the bed during the BD step can be different from that required to pressurize the other bed during the PR step [25].

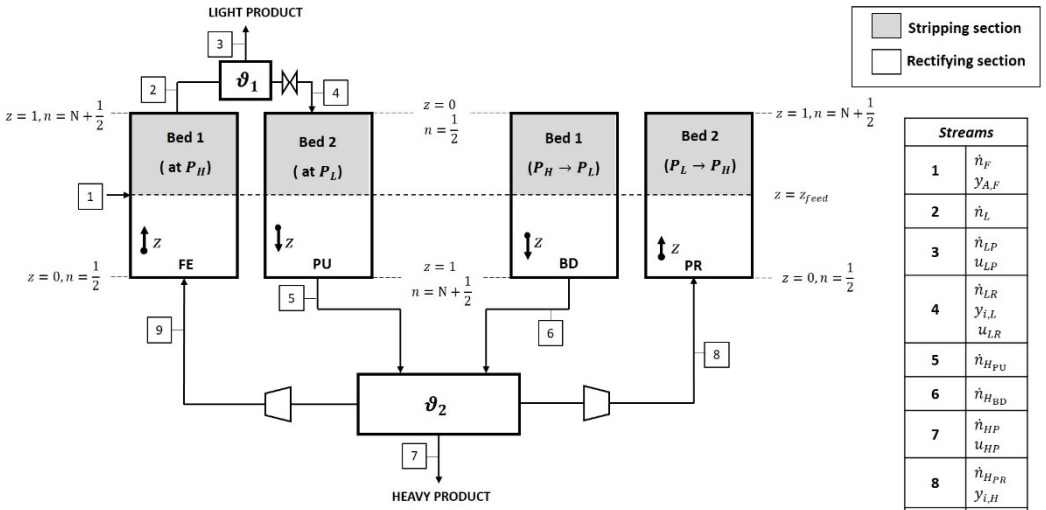

Figure 1: Process simulation sketch.

Further detailing the process cycle, a molar flowrate $\dot{n}_F$ (at molar fraction of A equal to $y_{A,F}$) is injected in Bed 1 at $z = z_F$ during the FE step at high pressure (P_H). Meanwhile, the other bed, Bed 2, is undergoing the PU step at low pressure (P_L). The stream enriched in light product leaving the top of Bed 1 with molar flowrate $\dot{n}_L$ is conveyed to tank ϑ_1. The composition (molar fractions $y_{i,L}$) in the light product stream, $\dot{n}_{LP}$, is the same as that of the stream recycled to the top of Bed 2 with molar flowrate $\dot{n}_{LR}$. Assuming large enough tank volume, such composition is evaluated as the cycle-averaged value of the molar fractions entering ϑ_1 [30].At the same time, the stream leaving Bed 2 during the PU step, $\dot{n}_{H_{PU}}$, is entering tank ϑ_2. Afterwards, the pressures of the two beds have to be exchanged: Bed 1 undergoes BD, with pressure reduction from P_H to P_L, while Bed 2 undergoes PR, with pressure increase from P_L to P_H. In the DR-PH-A configuration, this pressure swing occurs employing the heavy product stream, which leaves the *Rectifying section* of Bed 1 and enters the bottom of Bed 2. Namely, the gas (with molar flowrate $\dot{n}_{H_{BD}}$) flows from Bed 1 to tank ϑ_2, where it is mixed with the gas previously collected during the PU step. From ϑ_2, three streams exit, $\dot{n}_{HP}$, $\dot{n}_{HR}$ and $\dot{n}_{H_{PR}}$: the first is extracted as product, the second is recycled to the bed in FE step, and the third is sent to the bed in PR step. Once more, assuming large enough tank volume, the composition of all these streams is equal to $y_{i,H}$ evaluated as time-averaged molar fraction over the two steps BD and PU [30].

The process simulation has been carried out considering a single bed going through the sequence of steps required by the cycle, while the spatial coordinate is oriented according to the flow direction in each step, as shown in Figure 1. This implies that the z axis is oriented upward during the FE and PR steps, while downward during the BD and PU steps.

3. Mathematical model

The same 1-D DR-PSA mathematical model described in details elsewhere[30] has been applied, therefore the corresponding equations are only briefly summarized in the following. Equations (1-4) describe the process through the mass balance equations for each species i $(= 1 \dots N_C)$ in both gas and adsorbed phase, the overall mass balance equation and the pressure drop equation:

$$\epsilon_T \frac{\partial P}{\partial t} + \frac{\partial (uP)}{\partial z} + \rho_B RT \sum_{i=1}^{2} \frac{\partial q_i}{\partial t} = 0 \qquad (1)$$

$$\epsilon_T \frac{\partial (Py_i)}{\partial t} + \frac{\partial (uPy_i)}{\partial z} - \epsilon_B \left(\frac{\partial}{\partial z} D_L \left(\frac{\partial Py_i}{\partial z} \right) \right) + RT\rho_B \frac{\partial q_i}{\partial t} = 0 \qquad i = 1 \dots (N_C - 1) \qquad (2)$$

$$\frac{\partial q_i}{\partial t} = k_{LDF,i}(q_i^* - q_i) \qquad i = 1 \dots N_C \qquad (3)$$

$$\frac{\partial P}{\partial z} = -\frac{u}{\frac{150}{4}\frac{1}{r_p^2}\left(\frac{1-\epsilon_B}{\epsilon_B}\right)^2 \mu}. \qquad (4)$$

The extended Langmuir equation is considered as adsorption equilibrium model:

$$q_i^* = \frac{a_i P_i}{1+\sum_i b_i P_i}. \qquad i = 1 \dots N_C. \qquad (5)$$

Equations (1-4) represent a system of $(2N_C + 1)$ non-linear Partial Differential Equations (PDEs) whose unknown variables can be grouped in the state variable vector $S = [q_i, y_i, P]$. In the specific case under examination (binary systems), this vector is made of 5 elements only.

In order to describe the DR-PSA process, the aforementioned system of equations need to be numerically solved. Due to the nature of the process and the expected space-time behavior of the calculated variables (*i.e.*, sharp fronts propagating along the column axis), the numerical solution of such PDE system is quite challenging. In this work, we applied the Finite Volume Method (FVM): the spatial domain was discretized into a set of finite volumes while numerically solving in time the resulting set of Ordinary Differential Equations (ODEs) inside each discrete volume. To achieve an accurate solution in a reasonable computational time, a combination of interpolation schemes has been selected in order to simultaneously satisfy the following requirements: (i) speed and stability of the numerical solution, (ii) accurate representation of the involved physical phenomena, and (iii) careful reconstruction of sharp front profiles. The developed interpolation scheme exploits both first order upwind interpolations, Lagrange extrapolations and Van Leer Flux Limiters [26-29]. The resulting system of discretized equations is solved with the Boundary Conditions (BCs) summarized in Table S1, in the supporting information.

The generic simulation is performed starting from arbitrarily selected initial profiles of the state variables along the axial coordinate z. Note that, as already mentioned, the molar fractions $y_{i,L}$ and $y_{i,H}$ have been evaluated from the solution of the material balances of the two vessels, ϑ_1 and ϑ_2, under the assumption of large tank volume. Accordingly, the molar fractions of the streams leaving each vessel during a given time interval are well approximated by the molar fractions of the entering streams time-averaged over the same interval.

4. Description of the design procedure

Let us consider a binary mixture A - B, characterized by Langmuir adsorption isotherms. A simple design procedure could involve the approximation of such non-linear isotherms with two suitable linear isotherms that could be used to compute all the design parameters through the *Equilibrium Theory*. However, when using the design parameters suitable for linear isotherms, a loss in the separation performances of DR-PSA units is expected. The main idea of the proposed design strategy is that such performances can be recovered by changing a single process parameter: the pressure ratio of the process $\pi = P_H/P_L$. Namely, this quantity is tuned so that *the amount of each species adsorbed on the solid when the pressure changes from P_L to P_H in the Langmuir case matches to the one of the linear case*. This way, the separation performances are expected to become more similar in the two cases, thus recovering some equivalence between the linear case (where the estimated operating conditions ensure complete separation) and the adjusted Langmuir case (where the modified pressure ratio should provide better approach to a sharp separation). Accordingly, the proposed procedure is made of the following steps:

I. Set first-guess value of P_H and P_L, thus setting $\pi = P_H/P_L$;
II. Estimate the equilibrium parameters k_i of the "equivalent" linear isotherms by linear fitting of the Langmuir's isotherms inside the selected pressure range, $P \in [\,0, P_H]$;
III. Given the fitted values of the equilibrium constants, evaluate all the process parameters through the solution based on the *Equilibrium Theory*. Namely, is the three main parameters are $\mathbb{G}$ (the reflux ratio, proportional to the ratio between the light reflux and the feed flowrate), z_F (the feed injection position), and $\mathbb{C}_{max}$ (the maximum value of the capacity ratio, proportional to the ratio between the number of moles injected during the FE step and the volume of the column, *cf.* Bhatt et al. (2013)[20]).
IV. After selecting the operative value of $\mathbb{C} \in (0, \mathbb{C}_{max}]$ (usually smaller than the maximum to ensure process robustness), a new value of the low pressure, P_L^*, is calculated in order to ensure the same amount of each component adsorbed on the solid, in both the linear and Langmuir cases, when the pressure switches from P_H to P_L/P_L^*.

Let us test the reliability of the proposed procedure through a case study, corresponding to the separation of a binary mixture with Langmuir adsorption isotherms, as represented in Figure 2a by continuous lines (parameter values in Table S2, in the supporting information).

First, the two pressure values, P_H and P_L, are set ($P_H = 9\ bar$ and $P_L = 6\ bar$, respectively), thus leading to $\pi = 1.5$. Then, the two nonlinear isotherms are linearly fitted in the range $P \in [\ 0, P_H]$. The resulting values of equilibrium coefficients are in the supporting information, while the comparison between linear (dashed lines) and Langmuir's isotherms is shown in Figure 2a. The fitted parameter values correspond to $\beta = 0.53$. Using this value and considering equimolar feed composition (see the supporting information for the details of the parameters), the values of the three main design parameters $\mathbb{G}$, z_F, and $\mathbb{C}_{max}$ are calculated through the solution based on the *Equilibrium Theory*. Actually, this solution provides the so-called Triangular Operating Zone (TOZ, *cf.* Figure 2b) in the $z_F - \mathbb{C}$ plane: keeping constant the value of $\mathbb{G}$, any pair of values $\mathbb{C}$ - z_F inside the TOZ ensures complete separation of the binary mixture. Then, a $\mathbb{C}$ value smaller than $\mathbb{C}_{max}$ is arbitrarily selected inside the TOZ (in this case we set $\mathbb{C} = 0.08$, *cf.* Figure 2b).

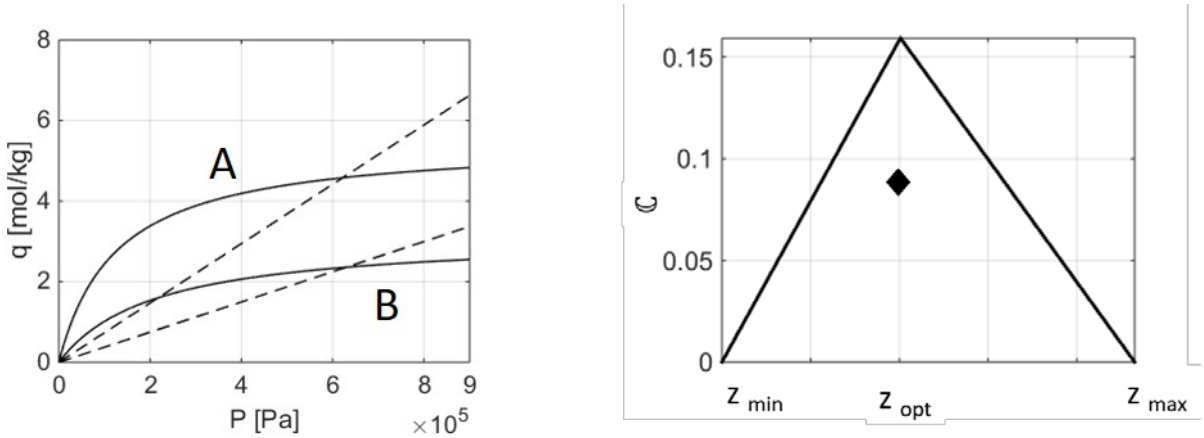

Figure 2: (a) Linear and Langmuir isotherms (continuous curves: nonlinear; dashed lines: linear); (b) TOZ for the binary case under examination.

To complete the specification of the process operating conditions, the values of 7 streams are needed: $\dot{n}_F, \dot{n}_H, \dot{n}_{HP}, \dot{n}_{HR}, \dot{n}_L, \dot{n}_{LP}$, and $\dot{n}_{LR}$. These variables are constrained by the material balances of each Bed (1 and 2) and tank (ϑ_1 and ϑ_2), which corresponds to 4 equations. Therefore, 3 degrees of freedom remains to complete the design procedure, which can be saturated by setting the values of the three streams $\dot{n}_F$, $\dot{n}_{HP}$, and $\dot{n}_{LR}$ given the $\mathbb{C}$ and $\mathbb{G}$ values from the *Equilibrium Theory* and the condition of complete separation. The final values of all the parameters of the case study (defined "base-case *C*" in the following) are summarized in Table S3, in the supporting information.

Using the parameter values along with the linear equilibrium isotherms selected, the mathematical model shortly presented in Section 3 predicts complete separation (that is, purity of both A and B equal to 100%). However, when the same operating conditions are applied in the nonlinear case,

the complete separation is dramatically lost and purity values for both the product streams of about 60% are predicted.

To recover such major loss of purity, an increase of the pressure ratio π is applied, whose value can be estimated *a priori* as follows. Let us define $\Delta q^*_{i,Hen}$ as the variation of equilibrium adsorbed concentration of the pure species i when varying the pressure from P_H to P_L according to the linear isotherm:

$$\Delta q^*_{i,Hen} = q^*_{i,Hen}(P_H) - q^*_{i,Hen}(P_L) \tag{6}$$

and $\Delta q^*_{i,Lan}$ the variation of the same concentration due to the change in the pressure from P_H to a modified value of low pressure, P^*_L, according to the Langmuir isotherms:

$$\Delta q^*_{i,Lan} = q^*_{i,Lan}(P_H) - q^*_{i,Lan}(P^*_L) \tag{7}$$

Of course, largely different values of $\Delta q^*_{i,Hen}$ and $\Delta q^*_{i,Lan}$ are found when selecting $P^*_L = P_L$,, as shown in Figure 3, being the linear values much larger than those corresponding to the nonlinear isotherm.

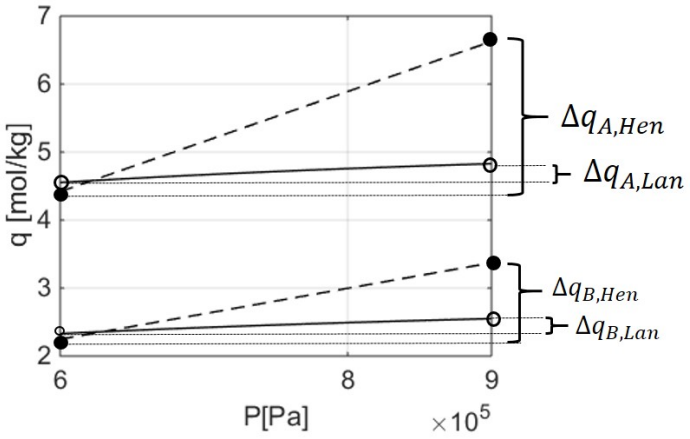

Figure 3: Δq^*_i for linear and nonlinear isotherms for both the components.

Then, new values of component-specific low pressure are evaluated in order to guarantee the equality $\Delta q^*_{i,Hen} = \Delta q^*_{i,Lan}$ while keeping constant P_H, namely:

$$P^*_{L,i} = \frac{k_i P_L + \left(\frac{a_i P_H}{1 + b_i P_H}\right) - k_i P_H}{\left(k_i P_H b_i - k_i P_L b_i - \frac{a_i P_H}{1 + b_i P_H} b_i + a_i\right)} \tag{8}$$

In general, the two values of $P^*_{L,i}$ are different (in this case $P^*_{L,A} = 1.1\ Pa$ and $P^*_{L,B} = 1.7\ Pa$). Since one single value can be set, an average value $P^*_L = \frac{P^*_{L,A}+P^*_{L,B}}{2} = 1.4 \cdot 10^5\ Pa$ is actually considered as a first guess. This new value of low pressure results in a major increase of the pressure ratio π, from the original value of 1.5 to about 6.5. Using the same model equations and parameter values previously applied for case C but with the modified value of low pressure, P^*_L, the loss of performances induced by the isotherm nonlinearity is largely recovered in terms of profile of y_A at the end of the FE step, achieving purity values larger than 95% in both product streams.

According to the previous simulation results, the pressure ratio appears to be the right parameter to be tuned in order to recover the loss of separation performances due to nonlinear equilibrium isotherms. Therefore, it is worth to further explore the applicability of this simple criterion, as discussed in the next Section.

5. Design procedure validation

The procedure developed above has been systematically applied to different study cases considering different extents of isotherm nonlinearity as well as different values of selected process parameters, namely $y_{i,F}$, π and β. All the analysed cases have been identified according to the coding sketched in Figure 4 while the detailed results of each case study are summarized in the supporting information.

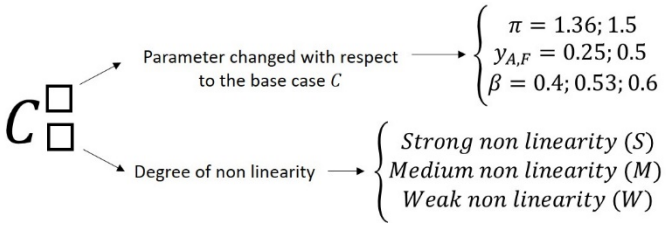

Figure 4: Coding applied to identify the different case studies.

The model presented in Section 3 was always applied in all cases. All the reported results fulfil the requirement of an average error on the overall material balance during step FE, defined as in Equation (9), smaller than 0.05%.

$$\varepsilon_{MB} = \left(\frac{\int_{t_0}^{t_{FE}} \dot{n}_F dt - \int_{t_0}^{t_{FE}} \dot{n}_{HP} dt - \int_{t_0}^{t_{FE}} \dot{n}_{LP} dt}{\int_{t_0}^{t_{FE}} \dot{n}_F dt} \right) 100. \quad (9)$$

5.1 Isotherms nonlinearity

Let us consider three cases, characterized by the equilibrium isotherms in Figure 5 (equilibrium parameters in Table S4, in the supporting information). In the same figure, the corresponding linearized isotherms are also shown, whose parameter values are in the supporting information, too. Note that a single linear isotherm applies to each component, so that the TOZ derived through the *Equilibrium Theory* is the same in all cases. As previously introduced, in this work, we consider a linear isotherm which is the linear least square approximation of the Langmuir isotherm in the interval $P \in [0, P_H]$. In order to have the same linear isotherm in each case investigated for each component, we arbitrarily set one of the Langmuir parameters, for example a_i, while the other is computed just imposing k_i as the linear least square approximation coefficient and, accordingly, b_i can be computed.

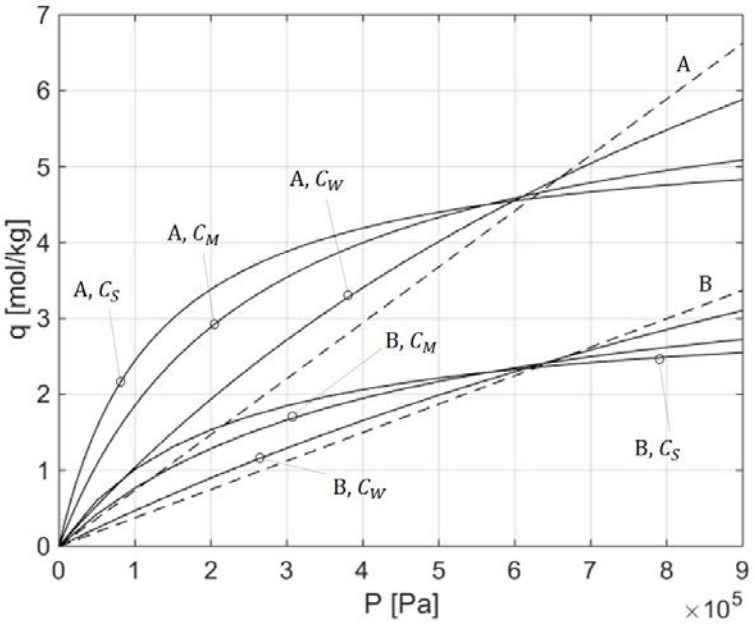

Figure 5: Linear (--) and nonlinear (-) isotherms for each case and component.

Setting $\pi = 1.5$, $y_{A,_F} = 0.5$, and $\beta = 0.53$, the corresponding TOZ is shown in Figure 2b. As anticipated, this applies in all cases since the same linear isotherms are considered. Accordingly, the same operating point is selected, characterised by $\mathbb{C} = 0.08$, $\mathbb{G} = 2.95$, and $z_F = 0.2$. The complete sets of operating parameter values for all the investigated cases are reported in the supporting information, while the values of P_L^* calculated as arithmetic average of the values from Equation (8) are summarized in Table 1. The corresponding values of pressure ratio are monotonously increasing

at increasing extent of nonlinearity (from $\pi = 1.5$ for the linear case, to about 1.9 for the weak nonlinearity case, to 3.8 for the medium nonlinearity case, and finally to 6.3 for the (previously discussed) strong nonlinearity case).

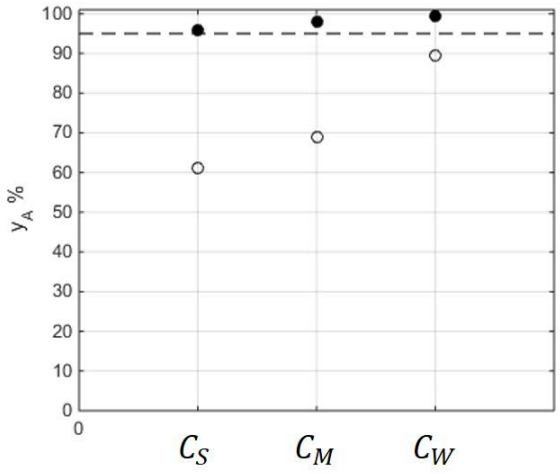

Figure 6: Purity of A predicted at P_L (○) and P_L^* (●). Role of degree of nonlinearity in the base case. The dashed line indicates 95% purity.

Table 1: P_L and P_L^* values for cases with varying nonlinearity, $y_{A,F}$ and π.

Case	P_H [Pa]	P_L[Pa]	P_L^* [Pa]
C_S	$9.00 \cdot 10^5$	$6.00 \cdot 10^5$	$1.43 \cdot 10^5$
C_M			$2.40 \cdot 10^5$
C_W			$4.69 \cdot 10^5$
$C_S^{\pi=1.36}$	$7.50 \cdot 10^5$	$5.50 \cdot 10^5$	$1.85 \cdot 10^5$
$C_M^{\pi=1.36}$			$2.81 \cdot 10^5$
$C_W^{\pi=1.36}$			$4.67 \cdot 10^5$
$C_S^{y_{A,F}=0.25}$	$9.00 \cdot 10^5$	$6.00 \cdot 10^5$	$1.43 \cdot 10^5$
$C_M^{y_{A,F}=0.25}$			$2.40 \cdot 10^5$
$C_W^{y_{A,F}=0.25}$			$4.70 \cdot 10^5$
$C^{\beta=0.4}$			$2.75 \cdot 10^5$
$C^{\beta=0.6}$			$2.75 \cdot 10^5$

The simulation results are summarized in Figure 6 in terms of purity of species A. Note that, being the feed equimolar, the purity of species B is the same as that of species A. As expected, a loss of purity always occurs due to the non-linearity of the isotherms when operating conditions estimated assuming linearized isotherms are directly applied: the stronger the nonlinearity, the larger the loss

of purity. However, this loss of purity can be fully recovered increasing the π value according to the proposed design procedure, with purity values above 95% in all cases.

5.2 Feed composition

In the base case C, the feed molar fractions were set equal to 0.5 for both the components. Setting $y_{A,F} = 0.25$ and leaving $\pi = 1.5$ and $\beta = 0.53$, the TOZ can be computed using the *Equilibrium Theory*, leading to $z_F = 0.20$, $\mathbb{C} = 0.08$ and $\mathbb{G} = 3.79$. All values of the operating parameters are reported in the supporting information, while the values of P_L^* are the same previously reported in Table 1, since they do not depend on the feed composition. The corresponding simulation results are summarized in Figure 7. Also in this case, the loss of purity found in the nonlinear case when using directly the π value predicted through the *Equilibrium Theory* in the linear case (purity values as low as 40%) are always fully recovered. Values larger than 95% for both components are evaluated when the pressure ratio is adjusted using the proposed procedure.

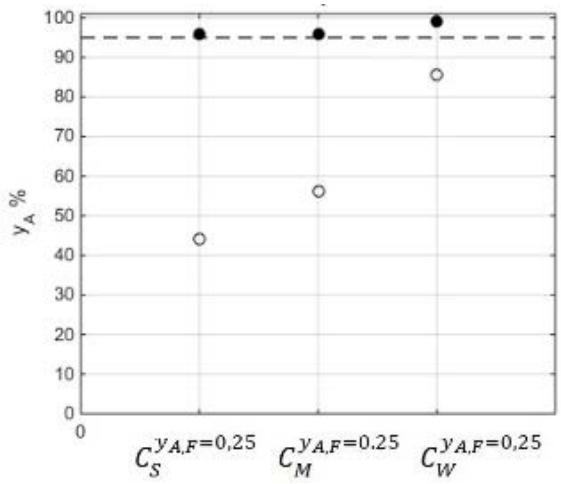

Figure 7: Purity of A predicted at P_L (○) and P_L^* (●). Role of the feed molar fraction, varying the non linearity degree. The dashed line indicates 95% purity

5.3 Pressure ratio

A value of the pressure ratio smaller than the base case ($\pi = 1.36$ instead of 1.5 in case C) has been considered, as reported in Table 1. A new TOZ was evaluated setting $y_{A,F} = 0.5$, $\beta = 0.53$ and the new value of π. The new operating point was identified as $\mathbb{C} = 0.08$, $\mathbb{G} = 3.74$ and $z_F = 0.22$, while the values of all the other operating parameters are summarized in the supporting information. When simulating the different situations using the value of P_L given in Table 1 (cases $C_S^{\pi=1.36}$, $C_M^{\pi=1.36}$, and $C_W^{\pi=1.36}$), loss of purity up to about 60% was found. On the other hand, repeating the simulations after setting the low pressure equal to the P_L^* values in Table 1, the level

of the separation is again recovered, with the purity of both products larger than 95%, as shown in Figure 8.

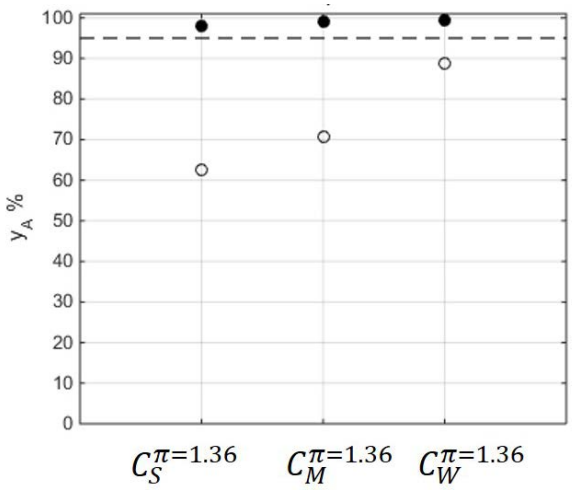

Figure 8: Purity of A predicted at P_L (○) and P_L^* (●). Role of pressure ratio, varying the non linearity degree. The dashed line indicates 95% purity

5.4 Selectivity

The influence of this parameter was performed considering smaller and larger β values with respect to the base case, $\beta = 0.4$ and $\beta = 0.6$, while leaving unchanged $\pi = 1.5$ and $y_{i,F} = 0.5$. After rearranging the β and β_i definitions, it is possible to compute the value of β_A (and, therefore, of k_A) for a given β value once the k_B value is kept constant as follows:

$$\beta_A = \beta \frac{1}{1+\rho_S R T k_B \left(\frac{1-\epsilon_T}{\epsilon_T}\right)}. \tag{10}$$

The parameter values of the linear isotherm estimated in this way are summarized in the supporting information. Also in this case, the parameter values of the Langmuir isotherm, a_i and b_i in the supporting information, have been estimated so that the linear isotherms corresponds to the linear least square approximation of the non-linear ones. The resulting isotherms are shown in Figure 9.

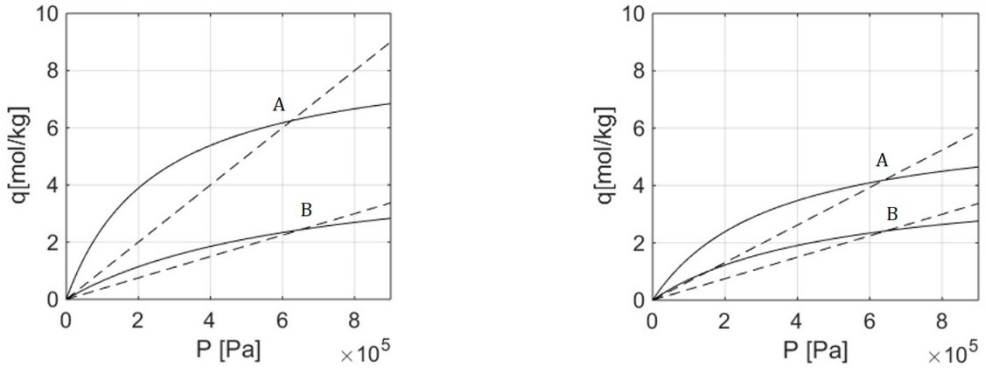

Figure 9: Linear (--) and nonlinear (-) equilibrium isotherms of both the components for a) case $C^{\beta=0.4}$ and b) $C^{\beta=0.6}$.

Different TOZs are calculated for each case and the corresponding process parameter values are summarized in the supporting information, together with the estimated P_L^* values. The purity values predicted by the model presented in Section 3 are as low as 70% when considering the original P_L values and nonlinear isotherms. However, as in all the previous cases, the purity can be recovered by reducing the value of the low pressure to the P_L^* values predicted using the proposed procedure, as shown in Figure 10. Once more, the complete set of the operating parameter values is summarized in the supporting information.

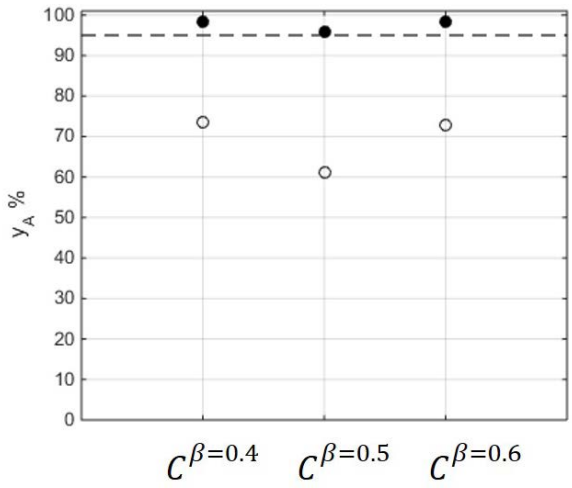

Figure 10: Purity of A predicted at P_L (○) and P_L^* (●). Role of the selectivity. The dashed line indicates 95% purity

6. Conclusions

Starting from an available strategy for the design of DR-PSA units based on the *Equilibrium Theory* and valid only for linear adsorption isotherms and complete separations, a modified design procedure applicable to the case of Langmuir isotherms is developed. Such a procedure is based on the use of the pressure ratio as tuning parameter to recover the separation performances expected

in the linear case. The tuning is based on equalization of the variations of adsorption loadings associated with the pressure change between the linear and nonlinear case.

By a series of parametric calculations, the proposed approach has been proved reliable for different levels of isotherm nonlinearity in a wide range of operating conditions, such as pressure ratio, feed composition, and adsorption selectivity. Using the parameter values estimated in the linear case in order to ensure complete separation, purity values larger than 95% have been obtained in all examined cases using the proposed strategy.

As final remark, it should be mentioned that the recovery of the separation performances is not coming for free. As a matter of fact, the pressure ratio affects the energy efficiency of the process and its impact on the process profitability should be considered[22,10] . When sharp separations with very high purity values are required, this procedure represents only an effective starting point for a fine-tuning of the operating conditions, which should be anyhow carried out through the usual trial-and-error approach.

Supporting information

In the supporting information, tables with the specific of the process parameters of each case investigated are reported. This information is available free of charge via the Internet at http://pubs.acs.org/.

Acknowledgment

Corresponding Author

*Tel.+39 0223993154. Fax: +39 0223993180. E-mail: renato.rota@polimi.it.

References

(1) Zhang, Y.; Saleman, T. L.; Li, G. K.; Xiao, G.; Young, B. R.; May, E. F. Non-isothermal numerical simulations of dual reflux pressure swing adsorption cycles for separating N2/CH4. *Chem. Eng. J.* **2016**, 366-381.

(2) Mofarahi, M.; Shokroo, E. J. Comparison of two pressure swing adsorption processes for air separation using zeolite 5A and zeolite 13X. *Petroleum & Coal* **2013***, 3*.

(3) Kidnay, A. J.; Parrish, W. R.; McCartney, D. G. *Fundamentals of natural gas processing;* CRC Press: 2011; Vol. 218.

(4) Grande, C. A. Advances in pressure swing adsorption for gas separation. *ISRN Chemical Engineering* **2012**.

(5) Skarstrom, C. W. Use of adsorption phenomena in automatic plant-type gas analyzers. *Ann. New York Acad. Sci.* **1959***, 13,* 751-763.

(6) Ebner, A. D.; Ritter, J. A. Equilibrium theory analysis of rectifying PSA for heavy component production. *AIChE J.* **2002***, 8,* 1679-1691.

(7) Yoshida, M.; Ritter, J. A.; Kodama, A.; Goto, M.; Hirose, T. Enriching reflux and parallel equalization PSA process for concentrating trace components in air. *Ind Eng Chem Res* **2003***, 8,* 1795-1803.

(8) Leavitt, F. W. Duplex Adsorption process. *US Patent 5,085,674* **1992**.

(9) Kearns, D. T.; Webley, P. A. Modelling and evaluation of dual-reflux pressure swing adsorption cycles: Part I. Mathematical models. *Chem. Eng. Sci.* **2006***, 22,* 7223-7233.

(10) Kearns, D. T.; Webley, P. A. Modelling and evaluation of dual reflux pressure swing adsorption cycles: Part II. Productivity and energy consumption .*Chem. Eng. Sci.* **2006***, 22,* 7234-7239.

(11) Diagne, D.; Goto, M.; Hirose, T. Experimental study of simultaneous removal and concentration of CO2 by an improved pressure swing adsorption process. *Energy Convers. Manage.* **1995***, 6-9,* 431-434.

(12) Mcintyre, J. A.; Ebner, A. D.; Ritter, J. A. Experimental study of a dual reflux enriching pressure swing adsorption process for concentrating dilute feed streams. *Ind Eng Chem Res* **2010***, 4,* 1848-1858.

(13) Mc Intyre, J. A.; Holland, C. E.; Ritter, J. A. High enrichment and recovery of dilute hydrocarbons by dual-reflux pressure pressure-swing adsorption. *Ind Eng Chem Res* **2002***, 14,* 3499-3504.

(14) Bhatt, T. S.; Sliepcevich, A.; Storti, G.; Rota, R. Experimental and modeling analysis of dual-reflux pressure swing adsorption process. *Ind Eng Chem Res* **2014***, 34,* 13448-13458.

(15) Saleman, T. L.; Li, G. K.; Rufford, T. E.; Stanwix, P. L.; Chan, K. I.; Huang, S. H.; May, E. F. Capture of low grade methane from nitrogen gas using dual-reflux pressure swing adsorption. *Chem. Eng. J.* **2015**, 739-748.

(16) Li, D.; Zhou, Y.; Shen, Y.; Sun, W.; Fu, Q.; Yan, H.; Zhang, D. Experiment and simulation for separating CO2/N2 by dual-Reflux Pressure Swing Adsorption configurations. *Chem. Eng. J.* **2016**, 315-324.

(17) May, E. F.; Zhang, Y.; Saleman, T. L. H.; Xiao, G.; Li, G. K.; Young, B. R. Demonstration and optimisation of the four Dual-Reflux Pressure Swing Adsorption configurations. *Sep. Purif. Technol.* **2017**, 161-175.

(18) Shen, Y.; Zhou, Y.; Li, D.; Fu, Q.; Zhang, D.; Na, P. Dual-reflux pressure swing adsorption process for carbon dioxide capture from dry flue gas. *International Journal of Greenhouse Gas Control* **2017**, 55-64.

(19) Tian, C.; Fu, Q.; Ding, Z.; Han, Z.; Zhang, D. Experiment and simulation study of a dual-reflux pressure swing adsorption process for separating N2/O2. *Sep. Purif. Technol.* **2017**, 54-65.

(20) Bhatt, T. S.; Storti, G.; Rota, R. Optimal design of dual-reflux pressure swing adsorption units via equilibrium theory. *Chem. Eng. Sci.* **2013**, 42-55.

(21) Bhatt, T. S.; Storti, G.; Denayer, J. F. M.; Rota, R. Optimal design of dual-reflux pressure swing adsorption units via equilibrium theory: process configurations employing heavy gas for pressure swing. *Chem. Eng. J.* **2017**, 385-406.

(22) Sivakumar, S. V.; Rao, D. P. Modified duplex PSA. 2. sharp separation and process intensification for N2-O2-5A zeolite system. *Ind Eng Chem Res* **2011***, 6,* 3437-3445.

(23) Kim, S.; Ko, D.; Moon, I. Dynamic optimization of a Dual Pressure Swing Adsorption Process for Natural Gas Purification and Carbone Capture *Ind Eng Chem Res* **2016***, 48,* 12444-12451.

(24) Kearns, D. T.; Webley, P. A. Application of an adsorption non-flow exergy function to an exergy analysis of a pressure swing adsorption cycle. *Chem. Eng. Sci.* **2004***, 17,* 3537-3557.

(25) Sivakumar, S. V.; Rao, D. P. Modified duplex PSA. 1. sharp separation and process intensification for CO2-N2-13X zeolite system. *Ind Eng Chem Res* **2011***, 6,* 3426-3436.

(26) Webley, P. A.; He, J. Fast solution-adaptive fiite volume method for PSA/VSA cycle simulation; 1 single step simulation. *Comput. Chem. Eng.* **2000***, 11-12,* 1701-1712.

(27) LeVeque, R. J. *Finite volume methods for hyperbolic problems;* Cambridge university press: 2002; Vol. 31.

(28) Casas, N.; Schell, J.; Pini, R.; Mazzotti, M. Fixed bed adsorption of CO2/H2 mixtures on activated carbon: Experiments and modeling. *Adsorpt* **2012***, 2,* 143-161.

(29) Haghpanah, R.; Majumder, A.; Nilam, R.; Rajendran, A.; Farooq, S.; Karimi, I. A.; Amanullah, M. Multiobjective optimization of a four-step adsorption process for postcombustion CO2 capture via finite volume simulation. *Ind Eng Chem Res* **2013***, 11,* 4249-4265.

(30) Rossi, E.; Storti, G.; Rota, R. A Finite Volume based model for simulating Dual Reflux-Pressure Swing Adsorption processes. Submitted to *Chem Eng Sci* **2018**.